Thermally-activated flow in nominally binary Al-Mg alloys

G.P.M. Leyson[a,*], W.A. Curtin[b]

[a]*Max-Planck-Institut für Eisenforschung GmbH, Düsseldorf 40237, Germany*
[b]*Institute of Mechanical Engineering, École Polytechnique Fédéral de Lausanne, Lausanne CH-1015, Switzerland*

Abstract

The temperature-dependent flow behavior in nominally binary Al-Mg alloys measured recently [1, 2] is interpreted in the context of a parameter-free solute strengthening model. The recent measurements show consistently higher strengths as compared to literature data on true binary Al-Mg alloys, which is attributed to the presence of Fe in the nominally binary Al-Mg. Using the Fe concentration as a single fitting parameter, the model predictions for the newer materials when treated as Al-Mg-(Fe) alloys agree with experiments to the same degree as obtained for the true binary Al-Mg. The model then predicts the activation volume in good agreement with experimental trends.

In interpreting experimental data for strengths of Al alloys, multiple mechanisms operating simultaneously are often invoked because the application of simple or ad-hoc theories does not explain observed trends. For instance, Hall-Petch effects [2], anomalous athermal stresses [6], solute clustering [6, 7], and/or unphysical dislocation/solute interactions [8–10], have been invoked to justify deviations between various solute strengthening theories [8–12] and experimental data. However, such reasonable attempts to rationalize experimental data obfuscate the relevant underlying mechanisms. Here we re-examine recent data on a set of nominally binary Al-Mg alloys first reported by Jobba *et al.* [1] and then further analyzed by Niewczas *et al.* [2]. We show that the finite-temperature flow behavior of the alloys in these works can be explained by the inclusion of a low concentration of Fe without the need to invoke any other additional mechanisms.

The solute strengthening model was developed in Refs. [13, 14] and only key points are summarized here. When moving through a random field of solutes with concentration c, an initially straight dislocation can lower its energy by bowing into regions containing favorable solute configurations and bowing away from regions with unfavorable solute configurations. The segments thus reside in favorable solute configurations and require stress- and thermally-driven activation to escape and move to the next favorable environment. The characteristic energy barrier ΔE_b for pinned segments is

$$\Delta E_b = 1.22\left(\frac{w_c^2\Gamma\Delta\tilde{E}_p^2(w_c)}{b}\right)^{\frac{1}{3}}c^{\frac{1}{3}}, \qquad (1)$$

where Γ is the line tension of the dislocation and b is the Burgers vector magnitude. The quantity $\Delta\tilde{E}_p(w_c)$ is related to the standard deviation of the overall solute/dislocation interactions as the dislocation segment moves a distance w_c through the random solute field of concentration c, and w_c is the characteristic roughening amplitude emerging from the theory. The characteristic stress required to move the dislocation segment over the energy barrier at zero temperature is

$$\tau_{y0} = 1.01\left(\frac{\Delta\tilde{E}_p^4(w_c)}{\Gamma b^5 w_c^5}\right)^{\frac{1}{3}}c^{\frac{2}{3}}. \qquad (2)$$

If w_c is the same for different solutes, then the energy barrier and zero temperature flow stress for the alloy with q different solute types in solution is

$$\Delta E_b = \left[\sum_q \left(\Delta E_b^q\right)^3\right]^{\frac{1}{3}}, \ \tau_y 0 = \left[\sum_q \left(\tau_{y0}^q\right)^{\frac{3}{2}}\right]^{\frac{2}{3}}, \qquad (3)$$

where the superscript q a quantity for solute q. For Al, w_c is nearly independent of solute type and so Eq. (3) can be applied to binary Al-Mg and nominally binary Al-Mg-(Fe) [14].

All quantities in Eqs. (1) and (2) are derived or material properties. First-principles calculations provide the key solute/dislocation interaction energies needed in the theory. The coefficients of the concentration scaling for the energy barrier and zero-temperature yield stress in Eqs. (1) and (2) are shown in Table 1 for Mg and Mn. In these results, the dislocation line tension Γ for Al is taken as 0.25 eV/Å, as derived from atomistic studies [15]; this value is lower than used in Ref. [14] but the same as that used in Ref. [13]. Also shown are the coefficients for Fe, which cannot be predicted by the theory and are instead obtained from experimental flow stress measurements on binary Al-Fe by Diak and Saimoto [16].

At finite temperatures, dislocation motion is thermally activated. At high stresses/low temperatures, the stress-dependent energy barrier $\Delta E(\tau)$ is

$$\Delta E(\tau) = \Delta E_b\left[1 - \frac{\tau}{\tau_{y0}}\right]^{3/2} \qquad (4)$$

At low stress or high temperatures, the energy barrier scales

Current Address: Max-Planck-Straße 1 40237 Düsseldorf Germany *Tel. No.*: +49 (0)211 6792 - 880
Email addresses: g.leyson@mpie.de (G.P.M. Leyson), william.curtin@epfl.ch (W.A. Curtin)

Table 1: Computed $T = 0$ yield stress τ_{y0} and energy barrier ΔE_b for Mg, Mn, and Fe solutes in Al, normalized by the appropriate solute concentration factor. Parameters in bold for Fe solutes are back-calculated from experimental data [16]. Note that these parameters differ from Ref. [14] due to the use of a more accurate line tension.

Solute	$\tau_{y0}/c^{2/3}$ (MPa)	$\Delta E_b/c^{1/3}$ (eV)
Mg	427	3.25
Mn	807	6.62
Fe	15,047	25.34

logarithmically with the applied stress [10, 17],

$$\Delta E(\tau) = 0.51\Delta E_b \ln\left(\frac{\tau_{y0}}{\tau}\right). \quad (5)$$

At quasistatic loading rates, transition state theory [18, 19] then connects the energy barrier $\Delta E(\tau)$ to the strain rate $\dot{\epsilon}$ and temperature T as

$$\dot{\epsilon}(\tau, T) = \dot{\epsilon}_\circ \exp\left(-\frac{\Delta E(\tau)}{kT}\right), \quad (6)$$

where k is the Boltzmann constant, $\dot{\epsilon}_\circ = \rho b d \nu_\circ$, ρ is the dislocation density per unit area, d is the flight distance over which the dislocation moves after each escape and $\nu_\circ$ is the attempt frequency. Equation (6) can be inverted to yield the finite temperature flow stress τ_y for a given strain rate $\dot{\epsilon}$ as

$$\tau_y(\dot{\epsilon}, T) = \begin{cases} \tau_{y0}\left[1 - \left(\frac{kT}{\Delta E_b}\ln\frac{\dot{\epsilon}_\circ}{\dot{\epsilon}}\right)^{\frac{2}{3}}\right] & \frac{\tau_y}{\tau_{y0}} \geq 0.5 \quad (7) \\ \tau_{y0}\exp\left(-\frac{1}{0.51}\frac{kT}{\Delta E_b}\ln\frac{\dot{\epsilon}_\circ}{\dot{\epsilon}}\right) & \frac{\tau_y}{\tau_{y0}} < 0.5 \quad (8) \end{cases}$$

The high and low stress (or low and high temperature) expressions above agree very well over the intermediate range of stress $0.3<\tau/\tau_y<0.6$ [14]. Here, as in all previous applications of this solute strengthening model, we use $\dot{\epsilon}_\circ = 10^4 s^{-1}$ [14, 17, 20]; the precise value has a small effect on the predictions.

A measurable quantity of importance in thermally-activated flow is the apparent activation volume $V(\dot{\epsilon}, \tau)$, defined as

$$V(\dot{\epsilon}, T) = -\frac{\partial \Delta E(\tau)}{\partial \tau}. \quad (9)$$

The activation volume is related to the area swept by the dislocation during the thermal activation process, and so is a sensitive measure of the length scales involved in the actual activation process. In the low-temperature regime,

$$V(\dot{\epsilon}, T) = \frac{3}{2}\frac{\Delta E_b}{\tau_{y0}}\left(\frac{kT}{\Delta E_b}\ln\frac{\dot{\epsilon}_\circ}{\dot{\epsilon}}\right)^{\frac{1}{3}}. \quad (10)$$

and the theory satisfies the "stress equivalency principle" [21].

We first demonstrate the quantitative predictions of the model by comparing to measured flow stresses in Al-Mg and Al-Mn binary alloys [7, 16, 22, 23]. Diak *et al.* have verified negligible concentrations of other elements, and in particular the Fe concentrations are below 3 ppm [16]. The single-crystals Al-Mg materials of Asada *et al.* were fabricated from 99.999% and so are also expected to have negligible Fe. The critically resolved yield stresses of single crystal Al alloys containing 1.1% and 3.3% Mg were measured by Asada *et al.* at a strain rate $\dot{\epsilon} = 4.2\times10^{-4}\ s^{-1}$ and various temperatures; we consider measurements between 78 K and 300 K to avoid other high-T phenomena (*e.g.* dynamic strain aging [5] and solute drag [24–26]). Diak *et al.* measured the flow stresses σ_y in uniaxial tension of two polycrystalline binary Al-Mg alloys at 78 K [7, 16] and of three binary Al-Mn alloys at 78–263 K [23], with $\dot{\epsilon} = 5\times10^{-5}\ s^{-1}$. In making predictions, we convert critical resolved shear stresses τ_y to equivalent uniaxial yield stresses σ_y by multiplying τ_y by the Taylor factor $M = 3.06$ [27] to put all results on the same footing.

The experimentally-measured yield stresses are shown versus the predicted yield stresses in Fig. 1(a) for the temperature range $78K-300K$. The model predictions agree well with experiments for the polycrystalline materials, and show a moderate overprediction for the single-crystal materials at lower temperatures. All predictions are within 30% with most predictions being within 15%. The deviations suggest that the model might overestimate the zero temperature yield stress τ_{y0} while underestimating the energy barrier ΔE_b. However, the model's parameters were derived from first-principles and are not adjustable. The polycrystalline results differ from earlier results [14] due to the use of the line tension derived from atomistic simulations [15], and this value of Γ actually makes the predictions slightly worse relative to the experiments.

In more recent studies, Jobba *et al.* have measured the yield stress of various Al-Mg alloys with concentrations ranging from 0.5–4.11% at 4 K, 78 K and 298 K at a strain rate $\dot{\epsilon} = 1.6\times10^{-4}$ [1, 2]. We make comparisons between theory and experiments at 78 K and 298 K since dynamic effects occur at temperatures near 0K [18]. These measured yield stresses are much larger than those found by Diak *et al.* or Asada *et al.* Similarly, the measured yield stresses are generally larger than those predicted by the model, especially when τ_y is small, as seen in Fig. 1(b). Jobba *et al.* also report rather high yield stresses for nominally pure Al (~ 12–18 MPa). The larger strengths measured by Jobba *et al.* and Niewaczs *et al.* would be inconsistent with a reduction in Mg in solution relative to the measured overall content, so here we use the stated Mg content as equal to the Mg concentration in solution. The similarity in measured strength between the ~3% Mg alloy and ~4% Mg alloy suggests, however, that the Mg in solution in the ~4% Mg alloy could in fact be closer to ~3%. The discrepancy between the previous literature results, which agree reasonably with the theory, and those reported in Refs [1, 2], which are rather larger, can be rationlized by the presence of dilute Fe solutes in the nominal binary Al-Mg alloys of Jobba *et al.* They reported that the as-fabricated alloys contain $\sim6\times10^{-4}$ Fe solute, of which an unknown amount is in solid solution. Here, we assume that there is some common concentration c_{Fe} of Fe in all of the materials studied by Jobba *et al.* and use c_{Fe} as a single fitting parameter for the yield stress.

For alloys containing both Mg and Fe solutes, the 0 K yield stress τ_{y0}^{eff} and energy barrier ΔE_b^{eff} are obtained from the alloy law of Eq. (3). We obtain c_{Fe} by minimizing the total relative

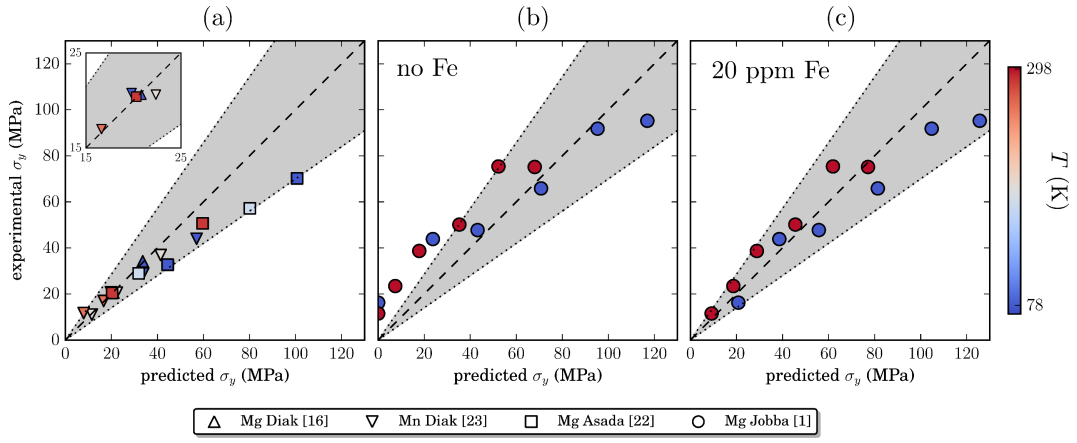

Figure 1: Predicted and experimental yield stresses in uniaxial tension σ_y for Al-Mg and Al-Mn alloys for various temperatures. Al-Mg alloys: Diak *et al.* [16] (△), Asada *et al.* [22] (□) and Jobba *et al.* [1] (◯). Al-Mn alloys: Diak *et al.* [23] (▽). The inset in (a) is a zoom of the figure for stresses between 15–25 MPa. The predictions in (b) are before Fe content $c_{\rm Fe}$ is taken into account, while those in (c) are with $c_{\rm Fe}$ = 20 ppm included. The dotted lines correspond to ±30% differences between predicted and experimental σ_y. Colors correspond to temperature at which τ_y was measured. The dashed line, with a slope of unity, corresponds to perfect agreement between predicted and experimental σ_y.

difference between theory and experiment given by over all experimental data points at both 78 K and 298 K. This yields an Fe concentration of $c_{\rm Fe}$ of 20 ppm and predictions of the model using this $c_{\rm Fe}$ for all the Al-Mg-(Fe) alloys are shown in Fig. 1(c). The fitted value of 20 ppm Fe is reasonably consistent with expectations based on the processing of the materials. With the inclusion of Fe solutes, the model predictions at 78 K show a slight overprediction of σ_y, consistent with trends observed from the Asada *et al.* data. Good agreement is also obtained for the nominally pure Al when treated as an Al-(Fe) binary system. Predictions at 298 K overestimate the experiments somewhat but are in reasonable agreement with the experiments. These results demonstrate that all yield stress data on nominally binary Al-Mg alloys can be brought into good agreement with each other, and good agreement with theory, if the materials studied by Jobba *et al.* are not true binary alloys and contain $c_{\rm Fe}$~20 ppm of Fe in solution.

Experimental data for V in the Al-Mg alloys as a function of the Mg concentration and finite-T shear yield strength $\tau_y = \sigma_y/M$ at 78 K has been presented by Diak and Saimoto [16] and by Niewczas *et al.* [2] using strain-rate jump tests. The experimental results and model prediction for V versus σ_y/M are shown in Fig. 2(a) in log-log form, where the two data sets from Niewczas *et al.* correspond to strain-rate jump tests with an increase (rise) and a decrease (drop) in the strain rate. In all cases, there is an approximate power-law scaling $V \sim \left(\sigma_y/M\right)^m$, with the predicted scaling of $m = -0.73$ in excellent agreement with those measured in experiments (−0.74 and −0.76 for the drop and rise case, respectively). The slope m deviates from the widely-quoted value of $-2/3$ because that scaling is only accurate at T=0 K. The full finite-T theory here predicts a slightly different scaling in excellent agreement with experiments. The magnitudes of the activation volumes differ among the three experiments. Neither the current model nor any other model, to our knowledge, can predict all three different sets of experimental results, but our model predictions fall in the middle of the experiments. Measurement of V can only be done indirectly, and thus resolution of the differences among the three experimental results remains an issue for experimental researchers.

The scaling of the activation volume V versus solute concentration is also of importance [28]. From Eqn. (10), the present theory for a binary alloy, *e.g.* Al-Mg, predicts a scaling of $V \sim c_{\rm Mg}^{-4/9}$ [7]. The experiment results of Niewczas *et al.* are shown in Fig. 2(b), and have a scaling of approximately $c_{\rm Mg}^{-0.3}$. The different scaling was taken as an indication that some other mechanism(s) or theories were operative in the strengthening. However, the presence of a dilute concentration of Fe changes the apparent scaling of V versus $c_{\rm Mg}$. Fig. 2(b) shows the predictions of V versus $c_{\rm Mg}$ for the Al-Mg-(Fe) alloy, and the apparent scaling is in excellent agreement with the experiments.

Jobba *et al.* [1] and Niewczas *et al.* [2] explored thermally-activated response of nominally binary Al-Mg alloys and reported deviations from basic solute strengthening theories. The solute strengthening was taken from the data of Asada *et al.*[22] on single-crystals, but with an incorrect Schmid factor so that the solute-strengthening contribution was underestimated. Specifically, they used a Schmid factor for the single-crystal experiments in Ref. [22] (~2.1) instead of the Taylor factor of 3.06 appropriate for equiaxed polycrystalline samples. To explain their measured strengths, they thus introduced an additional Hall-Petch strengthening with a Hall-Petch coefficient taken to be concentration-dependent, although all samples had the same grain size, and larger than those usually assumed for Al-Mg alloys. Thus, the strengths were fit and not predicted. Then, analyzing their results in this framework, they deduced that the theory of Leyson *et al.* [14], and scalings typically emerging from Labusch-type solute-strengthening theories [8–10], were not accurate. They thus postulated that models such as those by Fleischer [12] were needed to capture the scaling behavior.

Here, we have shown that the results of Jobba [1] and Niewczas *et al.* [2] for yield stress and scalings of the ac-

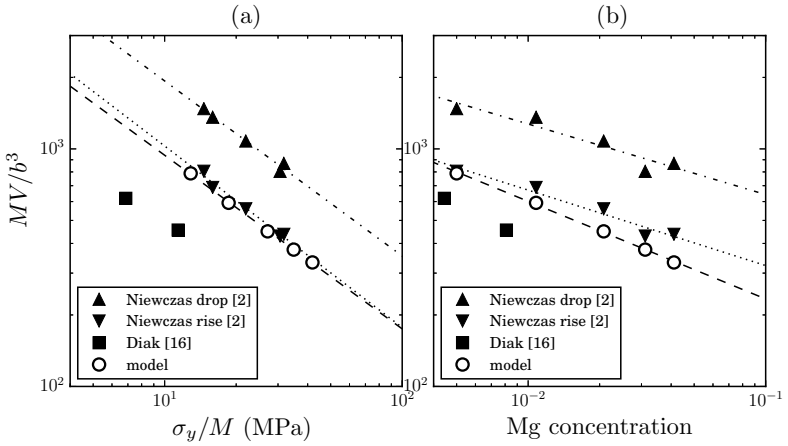

Figure 2: Normalized activation volume MV/b^3 versus (a) the critical resolved shear stress σ_y/M and (b) Mg concentration c_{Mg}, at 78K for various Al-Mg alloys as measured by Diak and Saimoto [16] and Niewczas *et. al* [2] and as predicted by the present model. The dashed-dotted, dotted and dashed lines are power-law fits to the Niewczas *et al.*(drop), Niewczas *et al.* (rise) and predicted activation volumes, respectively.

tivation volume can be explained within the solid solution strengthening model of Leyson *et al.* [14] under the assumption that these alloys contain a small but non-negligible amount of Fe in solution. No ad-hoc additions nor alternative theories are necessary. The robustness of the state-of-the-art solid solution strengthening theory is in fact further established. The theory does not address differences in the magnitude of the activation volume observed in various nominally-identical experiments, and this remains to be resolved. Nor do we address the post-yield work hardening, evolution of the activation volume with plastic strain, which were important parts of the studies by Jobba *et al.* and Niewczas *et al.* and require further investigation. However, such investigations must start from a clear understanding that the initial yielding and initial activation volume are well-understood. In addition, the pernicious role of dilute Fe in solution in commercial Al alloys must be recognized. Dilute Fe leads to strengthening and to changes in thermal activation behavior that are measurable and of practical relevance to the engineering application of these alloys. The underlying physical origins of this unusual strengthening remain as a puzzle that requires deeper study.

Acknowledgements

G.P.M.L is funded by a Postdoctoral Fellowship of the Alexander von Humboldt Foundation.

[1] M. Jobba, R. K. Mishra, M. Niewczas, International Journal of Plasticity 65 (2015) 43–60.
[2] M. Niewczas, M. Jobba, R. K. Mishra, Acta Materialia 83 (2015) 372–382.
[3] E. Pink, A. Grinberg, Acta Metallurgica 30 (1982) 2153–2160.
[4] R. C. Picu, G. Vincze, F. Ozturk, J. J. Gracio, F. Barlat, A. M. Maniatty, Materials Science and Engineering: A 390 (2005) 334–343.
[5] S. M. Keralavarma, A. F. Bower, W. A. Curtin, Nature Communications 5 (2014) 4604.
[6] T. H. Wille, W. Gieseke, S. C. H, Acta Metallurgica 35 (1987) 2697–2693.
[7] B. J. Diak, K. R. Upadhyaya, S. Saimoto, Progress in Materials Science 43 (1998) 223–363.
[8] R. Labusch, Physica Status Solidi B 41 (1970) 659–669.
[9] R. Labusch, Acta Metallurgica 20 (1972) 917–927.
[10] R. Labusch, G. Grange, J. Ahearn, P. Haasen, American Society for Metals, Cleveland, OH, 1975, p. 26.
[11] J. Friedel, Les Dislocations, Gauthier-Villars, Paris, p. 205.
[12] R. L. Fleischer, Acta Metallurgica 9 (1961) 996–1000.
[13] G. P. M. Leyson, W. A. Curtin, L. G. Hector Jr., C. F. Woodward, Nature Materials 9 (2010) 750–755.
[14] G. P. M. Leyson, L. G. Hector Jr, W. A. Curtin, Acta Materialia 60 (2012) 3873–3884.
[15] B. Szajewski, W. A. Curtin, submitted to MSMSE (2015).
[16] B. J. Diak, S. Saimoto, Materials Science and Engineering A-Structural Materials Properties 234 (1997) 1019–1022.
[17] G. P. M. Leyson, L. G. Hector Jr, W. A. Curtin, Acta Materialia 60 (2012) 5197–5203.
[18] A. S. Argon, Strengthening Mechanisms in Crystal Plasticity, Oxford University Press, USA, 2007.
[19] U. F. Kocks, A. S. Argon, M. F. Ashby, Progress in Materials Science 19 (1975) 1–281.
[20] M. Ghazisaeidi, L. G. Hector, W. A. Curtin, Acta Materialia 80 (2014) 278–287.
[21] Z. S. Basinski, R. A. Foxall, R. Pascual, Scripta Metallurgica 6 (1972) 807–814.
[22] H. Asada, R. Horiuchi, H. Yoshinaga, S. Nakamoto, Trans. J I M 8 (1967) 159–16.
[23] B. J. Diak, Private communication (2011).
[24] A. H. Cottrell, M. A. Jaswon, Proceedings of the Royal Society of London A 199 (1949) 104–114.
[25] H. Yoshinaga, S. Morozumi, Philosophial Magazine 23 (1971) 1367–1385.
[26] S. Takeuchi, A. S. Argon, Journal of Materials Science 11 (1976) 1542–1566.
[27] R. E. Stoller, S. J. Zinkle, Joural of Nuclear Materials 283 (2000) 349–352.
[28] D. Caillard, J. L. Martin, Thermally Activated Mechanisms in Crystal Plasticity, Pergamon, Amsterdam, 2007.